Hydrodynamic dispersion in a hierarchical network with a power-law distribution of conductances

Vladimir Alvarado
Oil and Gas Program, PUC-Rio, Rua Marquês de São Vicente, 225 - Gávea 22453-900, Rio de Janeiro - RJ - Brazil
(Received 25 November 2004; published 17 March 2005)

Dispersion is studied on a two-dimensional hierarchical pore network with a power-law distribution of conductances, i.e., $P(g) \sim g^{\mu-1}$, with $g \in (0,1)$, and μ is the disorderliness parameter ($\mu > 0$). A procedure for computing tracer dispersion transport on hierarchical networks was developed. The results show that the effective diffusion coefficient of the network scales similarly as conduction on the same lattice. This means that the disorder length scales for conduction and diffusion processes are the same, and can be predicted from percolation theory. The dispersivity, $\xi \equiv D_{\|}/U$, was found to diverge rapidly as $\mu \to 0$. The result is in agreement with the model developed by Bouchaud and Georges (C.R. Acad. Sci. (Paris) **307** 1431, 1988). A limiting value of $\mu \approx 0.45$ was found, below which the convection-dispersion equation is no longer valid.

DOI: 10.1103/PhysRevE.71.036304 PACS number(s): 47.55.Mh, 64.60.Ak, 89.75.Da, 61.43.Gt

I. INTRODUCTION

The transport of solutes through porous media has received considerable attention in the last decades, due in part to the necessity of carrying out cleanup operations of subsurface water reservoirs. Tracer dispersion has also driven investigation because it is often used as a tool for the characterization of oil and water reservoirs [1,2]. It has been known for some time that the conventional convection-dispersion equation does not always predict correctly the time evolution of solute plumes in porous media [3]. Often, the problem can be attributed to characteristics of the velocity fields, such as long correlation lengths on the order of or larger than the system size. This situation can be found in the highly heterogeneous distributions of hydraulic conductances, inherent to many porous media.

The general form of the convection-dispersion equation [4] is the following:

$$\frac{\partial C}{\partial t} + \mathbf{U} \cdot \boldsymbol{\nabla} C = \boldsymbol{\nabla} \cdot (\mathcal{D} \cdot \boldsymbol{\nabla} C), \tag{1}$$

where C is the mean local concentration of a solute, $\mathbf{U}$ corresponds to the Darcy velocity, and $\mathcal{D}$ is the dispersion tensor. Solute or tracer plumes that evolve as described by Eq. (1) are referred to as Gaussian [5]. In practice, this implies that the Central Limit Theorem holds, and the first two temporal moments contain all the statistical information on the plume [6]. It can be stated similarly for the spatial distribution.

The axial or longitudinal dispersion coefficient, i.e., the component of the tensor along the principal direction of the mean flow, depends in two distinct ways on the so-called Peclet number, defined as the ratio of diffusion to convection time scales ($\mathrm{Pe} = UL/D_m$) [4]. L is a typical length scale, for instance, the system size, and D_m is the diffusion coefficient of the tracer particle. For small values of Pe ($\mathrm{Pe} \ll 1$), the axial dispersion coefficient depends on molecular diffusion as $D_{\|} \propto D_m$ (or, more precisely, as $D_{\|} = D_m/\tau$, with τ being the tortuosity), whereas for $\mathrm{Pe} \gg 1$, but still in the creeping or linear flow regime, $D_{\|} = \xi U$. The latter defines the convective limit. The proportionality constant ξ is the so-called dispersivity, and it is a length scale in the system that is used to characterize the dispersion process. The dispersivity is usually related to the correlation length of the velocity field, which in turn originates in the permeability distributions.

A dispersion process described by Gaussian-like plumes usually requires homogeneous properties of a medium. This can be achieved in finite-difference formulations by enlarging the local simulation domain to contain sufficiently large samples, but issues on upscaling of the permeability field have to be faced. Violation of the system size requirements frequently leads to define position- and time-dependent transport coefficients, as the case of a dispersion coefficient in the convection-dispersion equation. An example can be found in systems at their conduction percolation threshold, because they do not exhibit a characteristic length scale [7]. That is also the case of systems with modeled fractal permeability fields, for which the transport coefficient grows without bound. Log-permeability fields have been found to behave as random fractals on scales ranging from 10 cm to 45 km [8]. Another way of exhibiting fractal properties is by having a non-Euclidean topology or connectivity [9].

The relevance of relating permeability length scales to analog quantities in dispersion problems is apparent. For this purpose, it is then necessary to study systems with well characterized conductivity length scales, for which scaling is well understood. For a highly heterogeneous system, the evaluation of transport properties should be inexpensive enough so that calculations can be carried out in large samples. Additionally, the computation of the dispersion coefficient should be realizable in those samples.

Angulo and Medina [10] performed renormalization calculations of the effective conductance on hierarchical networks. Bond conductance g was drawn from a power-law distribution $p(g) = \mu g^{\mu-1}$. The parameter μ can take either positive or negative values. This parameter controls the degree of heterogeneity of the medium, in a way that $\mu > 1$ approaches a homogeneous system, while $\mu \to 0$ is the most disordered case. These authors defined a disorder length ξ_D as the scale beyond which the system becomes effectively

homogeneous. As $\mu \to 0$, ξ_D was found to diverge with μ, with the following scaling form: $\xi_D \sim \mu^{-\nu}$. Exponent ν corresponds to the correlation length of ordinary percolation [7]. Hierarchical lattices, together with a power-law distribution of conductances, provide well characterized systems, for which heterogeneity properties of the conductance distribution are understood. Paredes and Alvarado [11] extended the renormalization analysis to the case of square networks. They demonstrated that a percolation analysis suffices to evaluate the strongest disordered limit of a family of distributions; i.e., in the critical region in the vicinity of $\mu = 0$. All of these indicate that studying conduction on hierarchical structures provides a means to determine the scaling behavior of the distribution of conductances. This well characterized system provides a highly heterogeneous conductance field, which is one of the ingredients for scale-dependent dispersion processes.

Giona *et al.* developed an exact renormalization theory for linear transport problems in fractal media [9,12], convection-diffusion being a special case in their formulation. Their main interest was the determination of exponents of anomalous diffusion in fractal supports. Their scheme is based on the discretization of the spatial differential operators, i.e., Laplace and gradient operators, and the solution to the Laplace transform of the resulting problem. The solution focuses, as in the work by Roux *et al.* [13], on the renormalized transfer function. However, the discussion in those works focused on cases with homogeneous conduction.

Cáceres studied non-Gaussian dispersion, the so-called anomalous dispersion, by using multistate continuous time random walk method [14]. The focus of Cáceres' research was the understanding of the Coats-Smith model that has been used for a long time to explain departure from Gaussian behavior. The process requires a volume of stagnant fluid in some pores of a given medium. In the present work, tracer dispersion is analyzed on a regular hierarchical lattice, with a power-law distribution of bond conductances. However, provided that all network bonds are aligned with the pressure gradient, then there is always non-negligible flow in all pores, in the limit of an infinite Peclet number. In this sense, non-Gaussian dispersion may be the result of the nature of the velocity distribution, which has been found to be fractal on certain supports [15].

Tracer dispersion is investigated on a Euclidean hierarchical lattice of effective dimension $d_e = 2$. The power-law distribution of conductances is appealing, because the disorder length scale for conductivity relates to the disorderliness parameter μ. The dispersion coefficient is computed for a wide range of Pe to show that in the hierarchical lattice, dispersion occurs much as in square networks, from the scaling viewpoint. Villermaux *et al.* showed this for a family of regular self-similar lattices without geometrical disorder [16]. As in the case of Villermaux *et al.*, the hierarchical lattice simulations should capture the controlling effects on mechanical dispersion due to the flow field associated to the pore-size distribution. Deviations from Gaussian behavior overall are proposed to come from the disorderliness of the porous medium in itself and not from the particular connectivity structure of the hierarchical lattice. Paredes and Alvarado [11] showed that care must be exercised in the analysis of hierarchical network results for the case of conduction, so that the appropriate percolation properties be considered. The same should hold for hydrodynamic dispersion.

Here, the scaling of a convection-dispersion process is studied in limits of $\mathrm{Pe} \to 0$ and $\mathrm{Pe} \to \infty$. The effective dispersion coefficient is determined from the first two moments of the transit-time distribution. In the limit of $\mathrm{Pe} \to 0$, the transport is expected to be controlled solely by molecular diffusion in the lattice. This process maps exactly on the conduction problem, and hence all that is known for conduction should apply in this limit. In the second limit of $\mathrm{Pe} \to \infty$, ξ is the selected quantity.

This article is divided into five sections. After Sec. I, the general method for obtaining moments of the residence-time distribution (RTD) is explained in Sec. II. Because the convective limit is a special case for the scheme of solution, Sec. III is devoted to a discussion of details of the procedure in this limit, which closely relates to that employed by Villermaux and Schweich [16]. Finally, the results are presented, followed by a discussion and conclusions.

II. GENERAL RECURSION EQUATIONS FOR TEMPORAL MOMENTS

This section describes the renormalization procedure for the generalized bond transfer function, from which one can derive the recursion equation for moments of the transit-time distribution. The proposed scheme is based on the solution of the transport problem by using a transfer-matrix algorithm [13]. The Laplace transform of the tracer flux through each bond can be written as follows:

$$\begin{pmatrix} -\tilde{j}(0,s) \\ \tilde{j}(l,s) \end{pmatrix} = \begin{pmatrix} a(s) & b(s) \\ c(s) & d(s) \end{pmatrix} \begin{pmatrix} \tilde{C}(0,s) \\ \tilde{C}(l,s) \end{pmatrix}, \tag{2}$$

where $-\tilde{j}(0,s)$ and $\tilde{j}(l,s)$ represent the transformed fluxes at the inlet and outlet of a bond, respectively, and $\tilde{C}(0,s)$ and $\tilde{C}(l,s)$ are the corresponding concentrations. Entries a, b, c, and d contain geometrical information and fluid flow properties.

Coefficients $a(s)$, $b(s)$, $c(s)$, and $d(s)$ are obtained at the zeroth level of the lattice from the exact solution to the Laplace transform of a local convection-diffusion equation, plus the assumption of complete nodal mixing. Henceforth, any linearly concentration-dependent contribution to the local transfer function can be incorporated into the formulation.

Figure 1 shows the main motif of the hierarchical structure used here. The network is constructed following a recursive procedure in which each bond (link) of the lattice is replaced by the main motif to produce the next level of the structure, as illustrated in the figure for three steps of this procedure. Mass conservation for an incompressible fluid yields the values of the pressure at the nodes and thereby the fluid fluxes (currents) along the bonds, as well as the effective conductance. It is assumed that the hydraulic conductance of a given bond is proportional to the square of its cross-sectional area; i.e., $g \sim A_s^2$. The latter permits one to

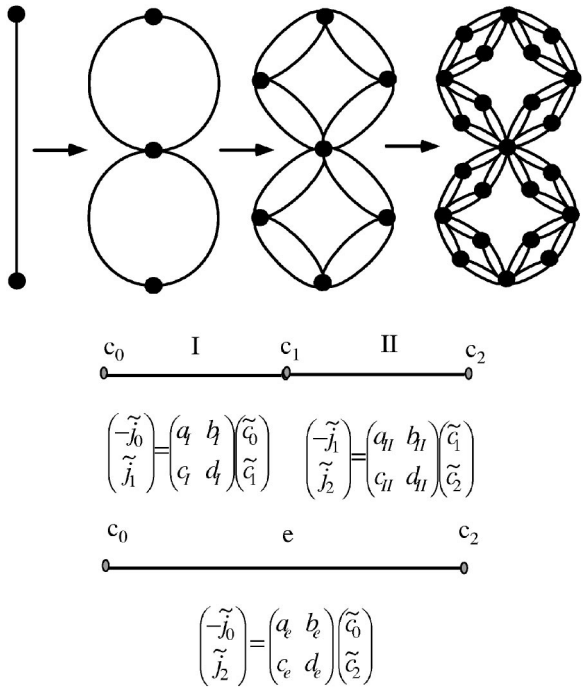

FIG. 1. Hierarchical lattice employed in this work. Top portion of the figure illustrates the iterative process to generate the network. The lower portion shows how the dispersion process is renormalized.

distribute the conductance alone (instead of A_s), and thereby to determine fluid flow velocity. For instance, $v_i \sim q_i / g_i^{1/2}$, where i is the bond index, and q_i and v_i the corresponding fluid current and mean conduit velocity. This is simply achieved by carrying out combinations in series and parallel of lattice bonds. All of this is necessary to determine the strength of the velocity field in the network for the subsequent solution of the bond transport equation.

Fluxes coming from adjacent bonds meeting at a node are additive (parallel combination in Fig. 1), so that their sum yields the transfer function. For those bonds in series, fluxes can be expressed in the following form for bond I:

$$\begin{pmatrix} -\tilde{j}_0 \\ \tilde{j}_1 \end{pmatrix} = \begin{pmatrix} a_I & b_I \\ c_I & d_I \end{pmatrix} \begin{pmatrix} \tilde{C}_0 \\ \tilde{C}_1 \end{pmatrix} \tag{3}$$

and similarly for bond II:

$$\begin{pmatrix} -\tilde{j}_1 \\ \tilde{j}_2 \end{pmatrix} = \begin{pmatrix} a_{II} & b_{II} \\ c_{II} & d_{II} \end{pmatrix} \begin{pmatrix} \tilde{C}_1 \\ \tilde{C}_2 \end{pmatrix}, \tag{4}$$

where $\tilde{j}_0$ is the transformed incoming flux to bond I, while $\tilde{j}_1$ is the exiting flux for the same bond. From mass conservation applied to the tracer, $\tilde{j}_1$ is the transformed incoming tracer flux for bond II. From Eqs (3) and (4), the value of $\tilde{C}_1$ can be eliminated by writing out the expressions for the fluxes:

$$\tilde{j}_1 = c_I \tilde{C}_0 + d_I \tilde{C}_1, \tag{5}$$

$$-\tilde{j}_1 = a_{II} \tilde{C}_1 + b_{II} \tilde{C}_2. \tag{6}$$

Now, the entering flux can be expressed in terms of the concentration values at the inlet and outlet nodes, respectively, $\tilde{C}_0$ and $\tilde{C}_2$:

$$-\tilde{j}_0 = \left(a_I - \frac{b_I c_I}{a_{II} + d_I} \right) \tilde{C}_0 + \left(- \frac{b_I b_{II}}{a_{II} + d_I} \right) \tilde{C}_2. \tag{7}$$

As a result, $a_e = [a_I - b_I c_I / (a_{II} + d_I)]$ and $b_e = [-b_I b_{II} / (a_{II} + d_I)]$. To find c_e and d_e, we proceed in a similar fashion, by putting $\tilde{C}_1$ into Eq. (4), as

$$\tilde{j}_2 = - \left(\frac{c_{II} c_I}{a_{II} + d_I} \right) \tilde{C}_0 + \left(d_{II} - \frac{c_{II} b_{II}}{a_{II} + d_I} \right) \tilde{C}_2, \tag{8}$$

which leads to $c_e = -c_{II} c_I / (a_{II} + d_I)$ and $d_e = d_{II} - c_{II} b_{II} / (a_{II} + d_I)$. Once the recursion equations for $a(s)$, $b(s)$, $c(s)$, and $d(s)$ are obtained, moments of the transit-time distribution can be derived from the Taylor series expansion of the Laplace transform of the exiting flux around $s = 0$.

The boundary condition at the inlet section of the entire network is $J_I(t) = \delta(t)$, such that $\tilde{J}_I = 1$. Hence, the Laplace transform of the exiting flux of tracers ($\tilde{J}_O$), is the transfer function or generator of moments for the whole network [17,18]. If all the moments are finite, one can carry out a series expansion of the form

$$\tilde{J}_O(s) = [\tilde{J}_O]_{s=0} + s \left[\frac{\partial \tilde{J}_O}{\partial s} \right]_{s=0} + \frac{1}{2} s^2 \left[\frac{\partial^2 \tilde{J}_O}{\partial s^2} \right]_{s=0} + \cdots. \tag{9}$$

Each term in the equation corresponds to a moment of the transit time distribution; i.e., [17]:

$$\langle t^n \rangle = (-1)^n \left[\frac{\partial^n \tilde{J}_O}{\partial s^n} \right]_{s=0}. \tag{10}$$

This formulation leads to recursion equations for the coefficients a, b, c, and d at different orders. In other words, one can write renormalization expressions for $a_e^{(n)}$, $b_e^{(n)}$, $c_e^{(n)}$, and $d_e^{(n)}$ by expanding the following expression:

$$\begin{pmatrix} -\tilde{j}_0(s) \\ \tilde{j}_2(s) \end{pmatrix} = \begin{pmatrix} a_e(s) & b_e(s) \\ c_e(s) & d_e(s) \end{pmatrix} \begin{pmatrix} \tilde{C}_0(s) \\ \tilde{C}_2(s) \end{pmatrix} \tag{11}$$

with respect to the parameter s. Once the expansion is performed, coefficients at each order in s are grouped together to obtain the renormalized coefficients at zeroth-, first-order, etc.

Let us recall that $C_O(s) = 0$, from the boundary condition at the outlet (a sink). The generator of moments is then determined as

$$-\tilde{J}_O(s) = \frac{c_e(s)}{a_e(s)} = \tilde{P}(s). \tag{12}$$

Finally, by carrying out the expansion on s of expression (12), any moment can be derived from the ratio $c_e(s)/a_e(s)$. For instance,

$$\langle t\rangle = \frac{a_e^{(1)}c_e^{(0)}}{(a_e^{(0)})^2} - \frac{c_e^{(1)}}{a_e^{(0)}}. \tag{13}$$

At the zeroth level in the hierarchy, $a(s)$, $b(s)$, $c(s)$, and $d(s)$ correspond to the following expressions:

$$a(s) = -m - m_s \coth m_s, \tag{14}$$

$$b(s) = \frac{m_s e^{-m}}{\sinh m_s}, \tag{15}$$

$$c(s) = \frac{m_s e^{m}}{\sinh m_s}, \tag{16}$$

$$d(s) = m - m_s \coth m_s, \tag{17}$$

where $m = \mathrm{Pe}/2$ and $m_s \equiv \mathrm{Pe}/2 + \sqrt{(\mathrm{Pe}/2)^2 + s}$. Notice that by construction, s as well as t are dimensionless (normalized by diffusion time l/D_m, where l is the bond length). As can be seen, the expressions involve hyperbolic functions as well as exponential. In order to deal with large and small Peclet numbers simultaneously, limiting formula for $a^{(n)}$, $b^{(n)}$, $c^{(n)}$, and $d^{(n)}$ as $\mathrm{Pe}\to 0$ and $\mathrm{Pe}\to\infty$ have been developed.

III. RECURSION EQUATIONS FOR LARGE PECLET NUMBERS

The evaluation of the transport properties using the most general expressions for $\langle t\rangle$ and $\langle t^2\rangle$, or $\langle \sigma_t^2\rangle$, is computationally expensive, even for hierarchical structures. Additionally, the value of Pe required to reach the limit $\mathrm{Pe}\to\infty$ puts a burden on numerics; e.g., round-off errors. Expressions for moments of the transit-time distribution can be simplified in the purely convective limit, because all bonds of the lattice have a nonzero fluid velocity, given that by construction all the bonds are oriented. Hence, a simpler renormalization recursion equation can be built, much on the line of the work done by Villermaux *et al.* [16].

For each bond in parallel arrangement (see Fig. 1), there is a volume fraction given by the ratio between the bond fluid flux and the total flux in the effective branch; i.e., $\omega_i = q_i/\Sigma_j q_j$ (q_j denotes the fluid flux through each bond in the arrangement). The effective transfer function for the particular network used here can be written upon renormalization as

$$G_e(s) = [\omega_1 G_1(s) + \omega_2 G_2(s)]\,[\omega_3 G_3(s) + \omega_4 G_4(s)] = \widetilde{P}(s), \tag{18}$$

or in a more general form,

$$G_e(s) = \prod_j \left(\sum_i \omega_i G_i\right)_j, \tag{19}$$

where the index i indicates a member of the set of branches in parallel arrangements, and j is for arrangements in series. Here, for instance, $\omega_1 = q_1/(q_1+q_2)$, and similarly for all other branches of the network. As shown in Eq. (18), the transfer function is the generator of moments for the RTD $[\widetilde{P}(s)]$.

Successive moments of the transit-time distribution, at a given stage of renormalization, can be obtained by taking derivatives of the renormalized transfer function with respect to the s parameter for $s=0$:

$$\mu_e^{(1)} = \langle t_e^n\rangle = (-1)^n \left(\frac{\partial^n G_e}{\partial s^n}\right)_{s=0}. \tag{20}$$

Following the last expression for $n=1$ leads to the mean transit time:

$$\mu_e^{(1)} = [\omega_1\mu_1^{(1)} + \omega_2\mu_2^{(1)}] + [\omega_3\mu_3^{(1)} + \omega_4\mu_4^{(1)}]. \tag{21}$$

The superscript denotes the order of the moment; i.e., $\mu_i^{(1)}$ is the first-order moment of the ith branch. In the expression above, the fact that $G_i(0)=1$ and also that

$$\left(\frac{\partial G_i}{\partial s}\right)_{s=0} = -\langle t_i\rangle$$

has been employed. In addition, from mass conservation, $\omega_1+\omega_2=1$. The recursion equation for the second moment takes the following form:

$$\mu_e^{(2)} = [\omega_1\mu_1^{(2)} + \omega_2\mu_2^{(2)}] + 2[\omega_1\mu_1^{(1)} + \omega_2\mu_2^{(1)}]\,[\omega_3\mu_3^{(1)} + \omega_4\mu_4^{(1)}] + [\omega_3\mu_3^{(2)} + \omega_4\mu_4^{(2)}]. \tag{22}$$

Mainly the first two moments of the RTD were evaluated, because in the convection-dispersion equation, the dispersion coefficient is independent of higher-order moments. At the zeroth level in the lattice, in the limit of $\mathrm{Pe}\to\infty$, all moments can be written as

$$\mu_i^{(n)} = (l_i/v_i)^n = [l_i/(q_i/\sqrt{g_i})]^n, \tag{23}$$

where l_i is the length of the ith branch (l is the same for all bonds). To show possible departure from Gaussian behavior, results of skewness are also obtained, for the limit of an infinite Péclet number. It is known that this central moment or cumulant should be zero for Gaussian processes [5]. From Eq. (18), the natural logarithm is taken, and then the successive derivatives with respect to s, evaluated at $s=0$, provide expressions for the cumulants, as follows:

$$\kappa_n = \left[\frac{\partial^n \ln G_e(s)}{\partial s^n}\right]_{s=0}, \tag{24}$$

where κ_n is the nth cumulant of $G_e(s)$.

However, it is easier to compute moments recursively, and then calculate the skewness from the first three moments as

$$\kappa_3 = \mu^{(3)} - 3\mu^{(2)}\mu^{(1)} + 2[\mu^{(1)}]^3. \tag{25}$$

IV. RESULTS

First, in the limit of low disorder ($\mu > 0.5$), the dispersion process is shown to occur as expected for regular networks [19]. This means that limits of $\mathrm{Pe}\to 0$ and $\mathrm{Pe}\to\infty$ are studied to determine whether moments of the transit-time distribution exhibit the expected dependence on system size and Péclet number; more specifically. $\langle t^n\rangle \sim L^{2n}$ (L in bond units), when $\mathrm{Pe}\to 0$. On the other hand, as $\mathrm{Pe}\to\infty$, moments of the distribution depend on Pe as $\langle t^n\rangle \sim \mathrm{Pe}^{-n}$, and with the system size as $\langle t^n\rangle \sim L^n$. It is also shown that the dispersivity reaches

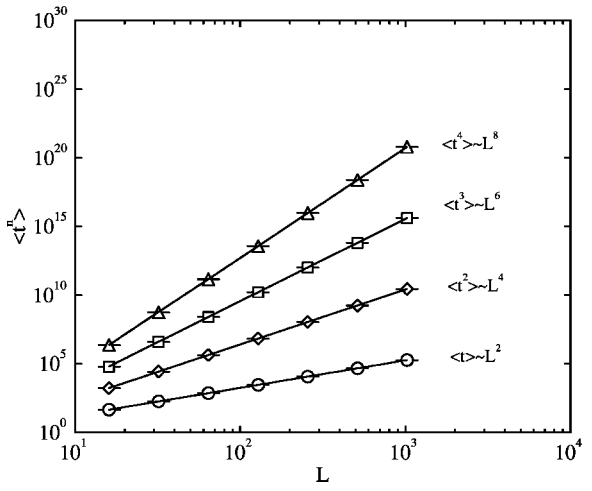

FIG. 2. First four moments of the transit-time distribution (Pe $=0$). The straight lines are power-law fits through the simulation points for different values of the system size ($L=2^k$, in bond units, l) and $\mu=1.0$. Temporal moments were normalized by the diffusion time l/D_m.

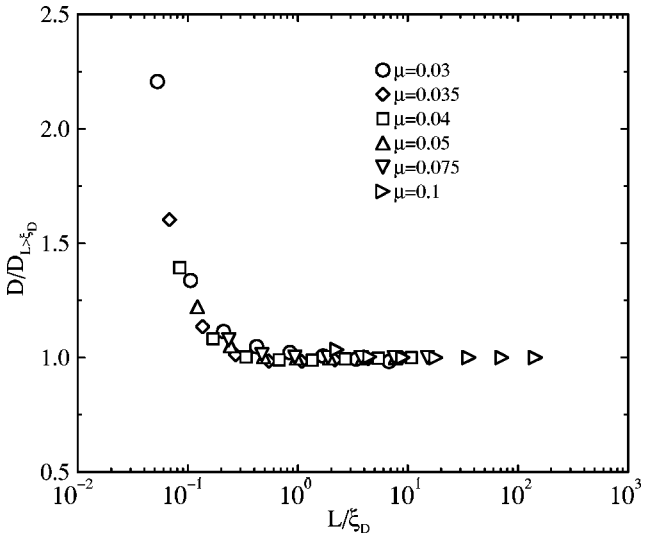

FIG. 3. Scaling of the diffusion coefficient. As expected, when the effective diffusion coefficient is normalized by using the asymptotic value of it (for $L>\xi_D$), all the curves collapse when the system size is normalized by using the disorder length of the conduction problem.

a constant value as $\mathrm{Pe}\to\infty$; in other words, that the ratio $D_\parallel/U$ becomes independent of the value of Pe.

Second, the scaling of the lattice effective diffusivity is examined, i.e., for $\mathrm{Pe}\to 0$, to show ξ as a function of μ in the limit $\mathrm{Pe}\to\infty$. Although the scaling of the dispersion process is of interest at any value of Pe, it is not dealt with in every regime with respect to Pe. Up to four moments of the transit-time distribution are computed; i.e., the values of $\langle t^n\rangle$ with $n=0$, 1,2,3,4, for various system sizes. The number of realizations varies depending on the network order.

In the simulations, $\mathrm{Pe}\equiv\langle U\rangle l/D_m$, where $\langle U\rangle$ is the volumetric average of the microscopic bond velocity in the network, and D_m corresponds to the tracer diffusion coefficient in the fluid (independent of concentration). Since we are working in the creeping flow regime, the Péclet number can be rescaled by multiplying bond velocities (or fluxes) by a constant factor [17]. In the limit of $\mathrm{Pe}\to 0$, the effective dispersion coefficient ($D_\parallel\sim D_m$) relates to the variance of the transit-time distribution σ_t^2 in a simple way [17]:

$$\lim_{Pe\to 0} D_\parallel = \frac{L^2}{\sqrt{6\sigma_t^2}}. \tag{26}$$

This relationship defines the diffusivity of the network. On the other hand, as $\mathrm{Pe}\to\infty$, in the absence of stagnation effects [16], the limiting expression connecting $D_\parallel$ with σ_t^2 is the following [16,17]:

$$D_\parallel = \sigma_t^2\frac{\langle U\rangle^3}{2L}, \tag{27}$$

or in terms of the Péclet number,

$$\xi \equiv \frac{D_\parallel}{\langle U\rangle} \sim \sigma_t^2\frac{Pe^2}{L}, \tag{28}$$

which defines dispersivity in this context. The result makes sense only when $D_\parallel$ is a linear function of velocity.

Low Péclet number limit (Pe→0)

Hierarchical networks of the type used here have a connectivity structure that differs from Euclidean networks. Therefore, not all nodes are equally important. This could affect the conclusions regarding scaling of transport properties in comparison with other networks. It will be shown that the hierarchical network yields normal results, which means that transport properties observed are a consequence of geometrical disorder alone (distribution of conductances), and not a topological feature (connectivity). When $\mu\approx 1$, networks are quite homogeneous, and hence a diffusion process should be a simple wandering through the lattice with not too different a probability of entering any bond (proportional to the cross-sectional area of the bonds). Figure 2 shows the first four moments of the transit-time distribution as functions of the system size ($\mu=1.0$). Diffusion being the controlling transport mechanism implies that $\langle t^n\rangle\sim(L^2/D_m)^n$, as depicted in the plot. These results were obtained at a value of Pe strictly equal to zero.

In previous works [10,11], the conductance of the network as a function of system size could be collapsed onto a single curve by rescaling G_e and L. This was achieved by using the asymptotic value of conductance (for $L\ll\xi_D$) and the disorder length, respectively. Diffusion and conduction processes map exactly onto one another, and hence the scaling of the diffusion process should be equal to that of conduction. To verify this, simulations have been carried to determine the effective diffusion coefficient at several values of μ (with $\mu\leqslant 0.1$). Figure 3 summarizes our findings. As expected, the disorder length turns out to be proportional to the correlation length of ordinary percolation. The relationship $\xi_D\sim\mu^{-\nu}$uses, with a value of $\nu=1.635$, the same divergence exponent of the percolation correlation length on this lattice.

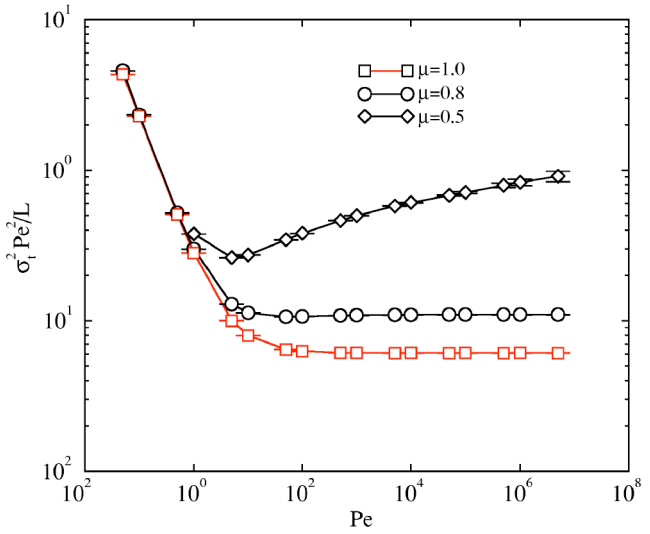

FIG. 4. The figure shows the transition from the diffusion controlled regime for dispersion to the convective limit for three values of μ. $L=1024l$. σ_t^2 and L are dimensionless.

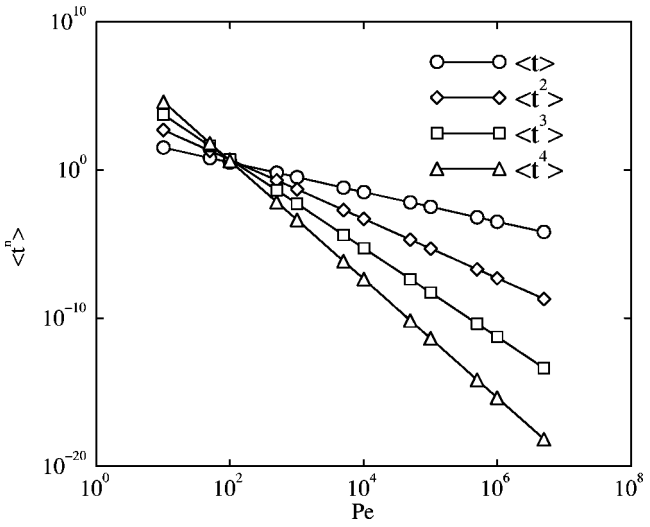

FIG. 5. Moments of the transit-time distribution in the limit $\mathrm{Pe}\to\infty$. $L=1024l$ and $\mu=0.8$.

It should not come as a surprise that the scaling region ($\mu < 0.4$) is similar to that found by Angulo and Medina [10].

High Péclet number limit ($\mathrm{Pe}\to\infty$)

To determine the transition from a diffusion-controlled transport towards a convection-dominated regime, simulations were carried out at values of μ away from $\mu=0$, and for lattices of various sizes. As the conductance distribution becomes wider, in a logarithmic sense, and more disorderliness appears in the network, the transition from pure diffusion to hydrodynamic convection exhibits a nonlinear region with respect to Pe that enlarges progressively before reaching the linear dependence on Pe [19], as depicted in Fig. 4. The latter reflects the fact that some regions of the lattice remain practically stagnant, while others are already in the convective limit. The smaller the value of μ, the larger the effect is, because a greater contrast of conduction exists in the system. From the figure, it is also observed that the values of the Péclet number required to fulfill the condition of a constant dispersivity grows larger with decreasing μ. At the same time, the dispersivity value grows rapidly with the disorderliness in the distribution of conductances. This turns out to be an indication of a possible divergence of ξ, as μ is diminished. Figure 5 depicts the expected dependence for moments of the RTD in the convective limit, $\langle t^n \rangle \sim (\mathrm{Pe})^{-n}$.

Expressions (21) and (22) were used to calculate dispersivity for several values of μ. Figure 6 depicts ξ as a function of μ, for three network sizes. A rapid divergence is observed for $\mu<0.4$. Notice that although ξ is a large for small values of μ, the curves corresponding to $L=256$ (network order equal to 8) and $L=4096$ (order 12) overlap. This means that the expected disorderliness is relatively small as compared to dispersivity. However, the standard deviation for ξ turns out to be too large to evaluate the disorderliness length, as was done for conduction [11].

One has to look into the features of the velocity distribution to understand the nature of the rapid divergence. It should be apparent that the contrast of transit time by convection is responsible for the spreading, in the purely convective limit. To investigate this, the shape of the velocity distribution was estimated from bond-velocity histograms. It has to be to recalled that in order to compute $D_{\|}$ in this limit ($\mathrm{Pe}\to\infty$), it was assumed that the fluid velocity was nonzero in all bonds. This condition can be realized only if the lowest value of the velocity in the network is large enough to satisfy the convective limit. As μ is set to be smaller, the velocity distribution widens or, said differently, the contrast between v_{min} and v_{max} grows. A large number of realizations, depending on lattice size, were accumulated to obtain relatively smooth and detailed histograms. However, the statistics for low velocity values do not have enough sampling, and therefore another indicator, Skewness, was calculated (shown later). Figure 7 represents histograms of velocity in logarithmic scale that clearly indicate ample distributions that approach a minimum of velocity in a power-law fashion. The flux distribution behaves similarly (not shown). The slopes of the linear part of the velocity histograms were fitted to yield $m\approx 1.87\mu$, but the meaning of this was not investigated.

Let us now look at model presented by Bacri *et al.* [20], originally developed by Bouchaud and Georges [21]. The model was also discussed in a review paper by Bouchaud and Georges [22], with similar conclusions. The proposed statistical model for dispersion can account for large contrast in convective paths and consists of a simple convective bypass. In the model, the dispersion coefficient (in the absence of diffusive paths) can be written in the following form (Bacri *et al.* [20]):

$$D_{\|} = \frac{\langle U \rangle}{2\beta}(1-\beta)^2(f+\beta-f\beta)\xi_c, \tag{29}$$

where β is the ratio between the smallest and largest velocity values in the system, and $(1-f)$ is the fraction of slow by-

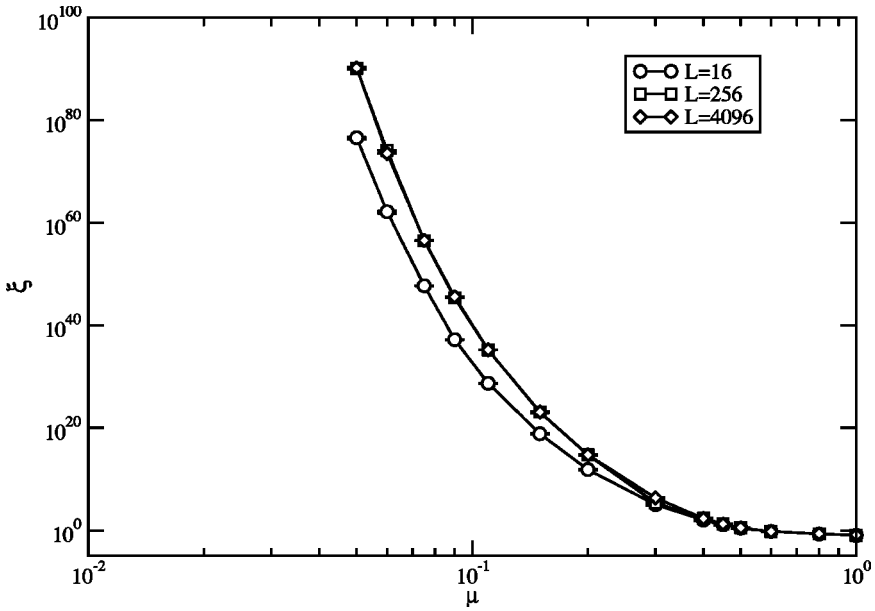

FIG. 6. Dispersivity as a function of μ. Insets show ξ as a function of network size. Both L and ξ are in bond units.

passes. ξ_c, on the other hand, is a typical correlation length of the bypasses, which is attributed to the disorder length of conduction. If β is a small number, then the dispersion coefficient becomes proportional to β^{-1}. Therefore, ξ can become a large number, as found in the simulations. The latter would explain the rapid divergence observed.

From the velocity distributions, the minimum and maximum velocities were recorded. The ratio was plotted versus μ to determine whether it behaves as ξ with respect to μ (Fig. 8). The resemblance with the result shown in Fig. 5 is striking, indicating that the velocity distribution contains most of the necessary information on the dispersion process.

A different way of looking at the trends observed for the dispersivity on the lattice is by analyzing higher moments of the RTD. As previously discussed, in order to be able to apply the convection-dispersion equation, the hydrodynamic dispersion process should be Gaussian. Henceforth, higher central moments should be zero, or else additional information would be required to describe the dispersion process. For this purpose, the skewness was calculated over a large number of realizations for several network sizes and values of μ. To compare adequately, the value of κ_3 was normalized by using $\langle t \rangle^3$; otherwise, the value of κ would depend on the pressure drop set in the calculations. The mean value of κ_3 should diminish as the network size is increased until reaching a vanishing value.

Figure 9 shows $\langle \log_{10}(\kappa_3) \rangle$ versus $\log(L)$ for several values of μ. The idea, rather taking the mean value of κ_3, was to show the mean order of magnitude and its trend as function of network size. Notice that for values of $\mu < 0.45$, κ_3 appears to diverge. A linear fit of $\log(\kappa_3)$ versus $\log(L)$ yields a very good correlation coefficient. In principle, a prefixed low value of κ_3 could be used to determine the necessary network size by extrapolating the trend. However, κ_3 does not de-

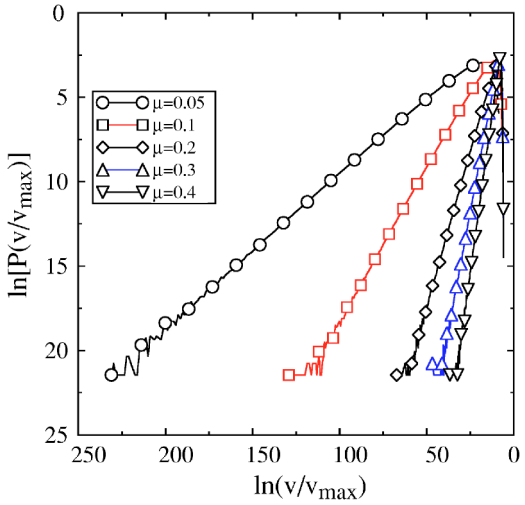

FIG. 7. Bond velocity distribution (histogram) at the zeroth level of the hierarchical network. The network size is 1024. The histogram was calculated over a large number of realizations for each value of μ.

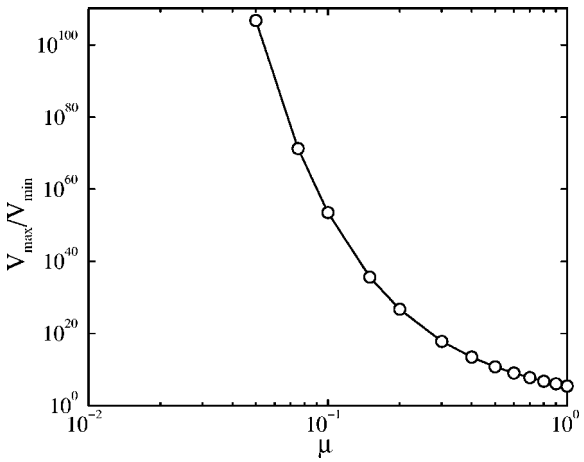

FIG. 8. Ratio between the largest value of fluid velocity in the network and smallest value of velocity versus μ. Network size is $1024l$.

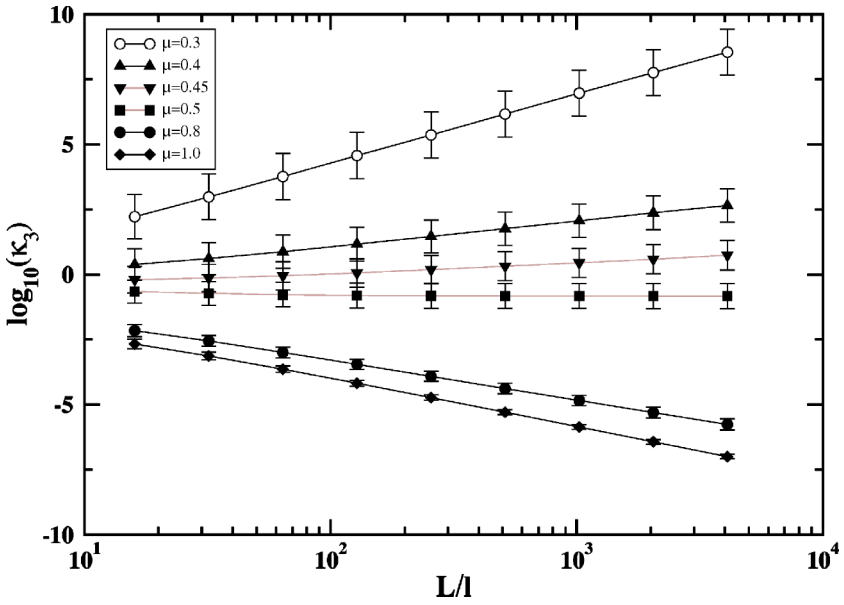

FIG. 9. $\mathrm{Log}_{10}(\kappa_3)$ (dimensionless) versus network size (L) for several values of μ, calculated in the limit of $\mathrm{Pe}\to\infty$.

crease with network size for $\mu<0.45$. This would add to the explanation as to why ξ diverges so rapidly for $\mu<0.4$.

V. CONCLUSIONS

A method for computing tracer dispersion transport was developed and implemented in this work. Limiting cases consisting of the purely diffusive limit, i.e., for $\mathrm{Pe}\to 0$, and the purely convective case, $\mathrm{Pe}\to\infty$, were also developed. The method translates into efficient algorithms for the computation of moments of the transit-time distribution in hierarchical lattices. To model geometrical disorderliness, a power-law distribution of conductances, $P(g)\sim g^{\mu^{-1}}$, with μ as the disorderliness controlling parameter, was used. In the limit of low disorderliness, when μ is unity, it was shown that the dispersion coefficient exhibits the same features observed in regular networks as a function of the Péclet number [19]. This means a diffusive behavior at low values of Pe, and a linear dependence with respect to Pe, as $\mathrm{Pe}\to\infty$. The transition from diffusion-controlled transport to convective transport was shown to depend strongly on the value of the disorderliness parameter. In the diffusion-dominated regime, as presumed from the exact mapping between diffusion and conduction, the diffusivity of the network reaches a constant value.

The disorder length of diffusion, with the power-law distribution of conductances, scales with the disorder parameter μ in the same way as the disorder length of conduction, i.e., $\xi_D\sim\mu^{-\nu}$, with ν the correlation length exponent of ordinary percolation. The scaling region of interest have been found to be the similar to that found for conduction by Angulo and Medina [10].

In the convective limit, the dispersivity reaches a constant value, independent of the Péclet number employed. However, the required value of Pe grows rapidly as the disorder parameter decreases to approach zero. The rapid divergence of ξ can be explained on the basis that the velocity field is extremely heterogeneous. The correspondence is found by using a model developed by Bouchaud and Georges *et al.* [21]. In the model, the ratio β between the smallest and the largest value of velocity yields the value of dispersivity (for $\beta^{-1}\gg 1$). It is found that β diverges similarly as ξ with the disorder parameter. However, the precise dependence with β is a function of the network structure, and the results was shown to indicate a trend.

In real geological media, a large value of dispersivity is frequently observed. However, the data shown here do not imply lack of homogeneity of the system, at least in terms of permeability or monophasic transport, but rather suggest a lack of validity of the transport equation. It was shown that, indeed, ξ reaches a constant value. The lack of convergence of the skewness suggests that the transport equation is invalid below a value of $\mu<0.45$. This means that for the lattice sizes simulated here, non-negligible higher central moments are to be found.

The results evidence that hierarchical networks can be used to study the effect of geometrical disorder; in particular, they can be employed to relate conduction properties to dispersion ones. However, some results cannot be directly extrapolated to regular lattices, because the nature of the velocity field depends on structure [23].

ACKNOWLEDGMENTS

Thanks go to Dr. Teresa Lehmann (URFJ) for critically reviewing the manuscript. The author would like to acknowledge MSc. Johnny Valbuena (PDVSA-Intevep) for programming routines used in this research. Thanks are due to Prof. Larry Lake (UT) for reviewing the article and for encouraging further analysis. The Gas and Oil Technology Group (GTEP) at PUC-Rio provided computer time to partially develop this work. The Brazilian National Petroleum Agency (ANP) provided funding through the PRH-007 program at PUC-Rio.

[1] B. Zemel, *Tracers in the Oil Field* (Elsevier, Amsterdam, 1995).
[2] G. Dagan, *Flow and Transport in Porous Formations* (Springer-Verlag, New York, 1989).
[3] J. H. Cushman, *Dynamics of Fluids in Hierarchical Porous Media* (Academic, New York, 1992).
[4] J. Bear, *Dynamics of Fluids in Porous Media* (Elsevier, New York, 1972).
[5] D. Zhan, *Stochastic Methods for Flow in Porous Media: Coping with Uncertainty* (Academic, San Diego, 2002).
[6] J. Honerkamp, *Stochastic Dynamical Systems: Concepts, Numerical Methods, Data Analysis* (VCH, New York, 1994).
[7] D. Stauffer and A. Aharony, *Introduction to Percolation Theory* (Taylor and Francis, London, 1991).
[8] S. P. Neuman, Water Resour. Res. **31**, 1455 (1995).
[9] M. Giona, W. A. Schwalm, M. K. Schwalm, and A. Adrover, Chem. Eng. Sci. **51**, 4717 (1996).
[10] R. Angulo and E. Medina, J. Stat. Phys. **75**, 735 (1994).
[11] Ricardo Paredes and V. Alvarado, Phys. Rev. E **58**, 771 (1998).
[12] M. Giona, W. A. Schwalm, M. K. Schwalm, and A. Adrover, Chem. Eng. Sci. **51**, 4731 (1996).
[13] S. Roux, C. Mitescu, E. Charlaix, and C. Baudet, J. Phys. II **19**, L687 (1992).
[14] M. O. Cáceres, Phys. Rev. E **69**, 036302 (2004).
[15] J. Adler, A. Aharony, R. Blumenfeld, A. B. Harris, and Y. Meir, Phys. Rev. B **47**, 5770 (1993).
[16] E. Villermaux and D. Schweich, J. Phys. II **2**, 1023 (1992).
[17] J. Koplik, S. Redner, and D. Wilkinson, Phys. Rev. A **37**, 2619 (1988).
[18] S. Redner, J. Koplik, and D. Wilkinson, J. Phys. A **20**, 1543 (1987).
[19] L. de Arcangelis, J. Koplik, S. Redner, and D. Wilkinson, Phys. Rev. Lett. **57**, 996 (1986).
[20] J. C. Bacri, J. P. Bouchaud, A. Georges, E. Guyon, J. P. Hulin, N. Rakotomalala, and D. Salin, in *Hydrodynamics of Dispersed Media*, edited by J. P. Hulin, A. M. Cazabat, F. Carmona, and E. Guyon (North-Holland, Amsterdam, 1990).
[21] J. P. Bouchaud and A. Georges, C. R. Acad. Sci., Ser. II, **307**, 1431 (1988).
[22] J. P. Bouchaud and A. Georges, Phys. Rep. **4–5**, 127 (1990).
[23] E. Duering and D. J. B. R. Blumenfeld, J. Stat. Phys. **67**, 133 (1992).